

Published in final edited form as:

*Hypertension*. 2010 January ; 55(1): 116–123. doi:10.1161/HYPERTENSIONAHA.109.135715.

## Lack of glutathione peroxidase-1 accelerates cardiac-specific hypertrophy and dysfunction in angiotensin II hypertension

**Noelia Ardanaz, Ph.D.** \*

Hypertension and Vascular Research Division, Henry Ford Hospital, Detroit, MI

**Xiao-Ping Yang, M.D.** \*

Hypertension and Vascular Research Division, Henry Ford Hospital, Detroit, MI

**M. Eugenia Cifuentes, Ph.D.**,

Dept. of Pharmacology and Chemical Biology, and #Vascular Medicine Institute, University of Pittsburgh School of Medicine, Pittsburgh, PA

**Mounir J. Haurani, M.D.**,

Hypertension and Vascular Research Division, Henry Ford Hospital, Detroit, MI

**Jackson W. Kyle, B.S.**,

Hypertension and Vascular Research Division, Henry Ford Hospital, Detroit, MI

**Tang-Dong Liao, Ph.D.**,

Hypertension and Vascular Research Division, Henry Ford Hospital, Detroit, MI

**Oscar A. Carretero, M.D.**, and

Hypertension and Vascular Research Division, Henry Ford Hospital, Detroit, MI

**Patrick J. Pagano, Ph.D.**

Dept. of Pharmacology and Chemical Biology, and #Vascular Medicine Institute, University of Pittsburgh School of Medicine, Pittsburgh, PA

### Abstract

Glutathione peroxidase-1 (Gpx1) plays an important role in cellular defense by converting hydrogen peroxide (H<sub>2</sub>O<sub>2</sub>) and organic hydroperoxides to non-reactive products and Gpx1<sup>-/-</sup> mice, which are characterized by reduced tissue glutathione peroxidase activity, are known to exhibit enhanced oxidative stress. Peroxides participate in tissue injury as well as the hypertrophy of cultured cells, yet the role of Gpx1 to prevent end organ damage in cardiovascular tissue is not clear. We postulated that Gpx1 deletion would potentiate both aortic and cardiac hypertrophy as well as mean arterial blood pressure (MABP) in response to angiotensin II (AngII). Our results show that short-term AngII markedly increased left ventricular mass, myocyte cross-sectional area and interventricular septum thickness and decreased shortening fraction in Gpx1<sup>-/-</sup> mice as compared to wildtype animals. On the other hand, AngII resulted in a similar increase in MABP in wildtype and Gpx1<sup>-/-</sup> mice. Collagen deposition increased in response to AngII but no differences were found between strains. Vascular hypertrophy increased to the same extent in Gpx1<sup>-/-</sup> and wildtype mice. Collectively, our results indicate that Gpx1 deficiency accelerates cardiac

---

Corresponding author (& reprint request address): Patrick J. Pagano, Ph.D., F.A.H.A., Department of Pharmacology & Chemical Biology And Vascular Medicine Institute, University of Pittsburgh School of Medicine, Room 10043, BST-3, 3501 Fifth Avenue, Pittsburgh, PA 15261, Phone: 412-383-6505, Fax: 412-648-9009, pagano@pitt.edu.

\*These authors contributed equally to this work.

### Disclosures

None

hypertrophy and dysfunction, but has no effect on vascular hypertrophy and MABP, and suggest a major role of Gpx1 in cardiac dysfunction in AngII-dependent hypertension.

## Keywords

Heart; angiotensin; hypertrophy; cardiac dysfunction; oxidant stress

---

## Introduction

Left ventricular hypertrophy (LVH) is an important risk factor for coronary heart disease, heart failure and stroke 1· 2. LVH involves changes in myocardial architecture consisting of myocyte hypertrophy and perivascular and myocardial fibrosis and there is a well-established link between LVH and high blood pressure. Factors such as age, sex, race, and stimulation of the renin-angiotensin-aldosterone system play important roles in the pathogenesis of LVH 3· 4, and angiotensin-converting enzyme inhibitors as well as angiotensin II (AngII) receptor antagonists are effective in the reduction of cardiac hypertrophy 5· 6. AngII is a prototypical stimulant of hydrogen peroxide (H<sub>2</sub>O<sub>2</sub>) and other reactive oxygen species (ROS) in cardiac and vascular cells 7, and H<sub>2</sub>O<sub>2</sub> has been shown to be a potent signaling agent in cardiomyocytes and vascular smooth muscle, promoting their hypertrophy *in vitro* and *in vivo* 7-9.

Glutathione peroxidase-1 (Gpx1), a ubiquitous peroxidase isoform, is a selenium-dependent enzyme that reduces cellular peroxides via their conversion to water and other non-reactive products 10. In Gpx knockout mice (Gpx1<sup>-/-</sup>) tissue Gpx activity is markedly reduced 11 and peroxide and ROS levels are elevated, which purportedly contribute to endothelial dysfunction and cardiac matrix deposition 12. Despite a well-established role of AngII to increase H<sub>2</sub>O<sub>2</sub> in the heart and aorta, the potential for AngII hypertension and cardiac and vascular remodeling to be accelerated in Gpx1<sup>-/-</sup> mice has not been studied. In this study, we postulated that Gpx1 deletion would potentiate aortic and cardiac hypertrophy as well as mean arterial blood pressure (MABP) elevation in response to AngII. The novel findings described herein illustrate that Gpx1 deletion promotes cardiac-specific hypertrophy and dysfunction without affecting vascular hypertrophy or blood pressure. These results suggest an important role for Gpx1 in initial cardiac hypertrophy and dysfunction in response to AngII.

## METHODS

### Animals

Male Gpx1<sup>-/-</sup> mice backcrossed to the C57Bl/6J background for greater than 10 generations were kindly provided by Dr. Y. Ho (Wayne State University) and bred at our institution. This study was approved by the Institutional Animal Care and Use Committee of Henry Ford Hospital and conforms to guidelines required by the National Institutes of Health.

### Radio-telemetry of Mean Arterial Blood Pressure

Eighteen- to twenty-week old mice were instrumented with transmitters as previously described 13 (an expanded Methods section can be found in the online supplement, please see <http://hyper.ahajournals.org>). Mean arterial blood pressure (MABP) and heart rate were continuously recorded and reported as 24-h means ± SEM.

### Vehicle or AngII Infusion

Mice were anesthetized with brexital (70 mg/kg, *i.p.*) to allow the subcutaneous implantation of osmotic minipumps (Alzet 1007D). Mice were implanted with minipumps infusing either vehicle or AngII (521 ng/kg\*min, *s.c.*) for 7 days.

### Preparation of Tissue Samples

On day 7, mice were anesthetized and the heart stopped during diastole. Mice were perfusion fixed under pressure and hearts and thoracic aortas removed. Total heart weight/body weight (THW/BW) ratio served as parameter of cardiac hypertrophy. The LV middle section and the descending thoracic aorta were processed and sectioned for analyses.

### Echocardiographic Evaluation of Cardiac Morphology and Function

Left ventricular wall thickness, dimensions and shortening fraction (SF) were evaluated with a Doppler echocardiograph equipped with a linear transducer as described previously<sup>14</sup>.

### Measurements of Interventricular Septum (IVST) and Left Ventricular (LV) Mass

LV mass was calculated according to the equation<sup>14</sup>:

$$LV\ mass = 1.055[(IVSTd + LVDd + PWT)^3 - (LVDd)^3]$$

where 1.055 is the specific gravity of the myocardium, IVSTd is diastolic interventricular septum thickness, LVDd is diastolic LV dimension, and PWT is diastolic posterior wall thickness.

### Cardiac Chamber Dimensions

End-diastolic and end-systolic LV dimensions (LVDd and LVDs), and diastolic interventricular septum thickness were measured from the M-mode tracings.

### LV Shortening Fraction

LV shortening fraction, a measure of LV systolic function, was calculated from the M-mode LV dimensions according to the equation: SF (%) = [(LVDd – LVDs)/LVDd × 100].

### Myocyte Cross-Sectional Area and Interstitial Collagen Fraction

6-µm heart sections were processed in Bouin's fluid overnight, washed, and incubated with 0.1% picrosirius red. Twenty one images of each left ventricle section were captured at 400 × magnification. Myocyte cross-sectional area (MCSA) and interstitial collagen fraction (ICF) were digitally recorded.

### Histological Examination of Mouse Thoracic Aortic Cross-Sections for Measurement of Vascular Remodeling

Sections were stained with Masson Trichrome Accustain as previously described<sup>15</sup>. Cross-sectional area (CSA), thickness of the media ( $W_m$ ) and external perimeter ( $P_e$ ) were digitally measured. Lumen diameter (L) was calculated according to the formula  $L = 2 \times [(P_e/2\pi)^2 - (CSA/\pi)]^{1/2}$ . Remodeling was determined by comparing the ratio of medial thickness to lumen diameter.

### Glutathione Peroxidase Activity and protein levels

Tissue homogenates were prepared in 50 mmol/L potassium phosphate, containing 1 mmol/L EDTA. Homogenates from aortic rings and heart tissue were centrifuged at 10,000

× g for 15 min at 4°C. Supernatants were assayed for protein and stored at -80°C. Glutathione peroxidase (Gpx) activity was determined using assay kit # FR 17 from Oxford Biomedical Research following the manufacturer's protocol. Gpx1 protein levels in heart homogenates were assessed by Western blots using rabbit antibody anti-Gpx1 (Abcam). Blots were probed with secondary antibody labeled with IRDye 800 and analyzed by the Odyssey Imager and its software (Li-Cor Biosciences).

### Data Analysis

Data are expressed as mean ± SEM. Comparisons between groups were made by analysis of variance, followed by Hochberg's method for multiple comparisons. A value of  $p < 0.05$  was considered statistically significant.

The authors had full access to the data and take responsibility for its integrity. All authors have read and agree to the manuscript as written.

## RESULTS

### Body weight and MABP

Mouse weights were approximately 30 g and did not vary with time or among treatment groups (data not shown). Basal MABP was similar between strains and remained unchanged in vehicle groups of both strains throughout the study (Figure 1). AngII caused a significant and sustained increase in MABP. No significant difference was observed between Gpx1<sup>-/-</sup> and wildtype infused with AngII (Figure 1). Heart rate in beats per minute (bpm) did not vary among treatment groups and strains of mice [705 ± 6.3 bpm (wildtype) vs. 691 ± 9.40 bpm (Gpx1<sup>-/-</sup>) for animals treated with vehicle, and 711 ± 8.33 bpm (wildtype) vs. 701 ± 11.7 bpm (Gpx1<sup>-/-</sup>) for animals treated with AngII].

### Cardiac Hypertrophy; Ratio of Total Heart to Body Weight

Large visible differences in heart size were observed in Gpx1<sup>-/-</sup> vs. wildtype mice infused with AngII as demonstrated by differences in heart cross-sections seen in Figure 2A – D. Figure 2, panels A and B correspond to representative heart cross-sections from wildtype mice treated with vehicle (wildtype + vehicle) and Gpx1<sup>-/-</sup> mice treated with vehicle (Gpx1<sup>-/-</sup> + vehicle), respectively, showing no significant difference among the strains. Figure 2, panels C and D correspond to representative heart cross-sections from wildtype mice treated with AngII (wildtype + AngII) and Gpx1<sup>-/-</sup> mice treated with AngII (Gpx1<sup>-/-</sup> + AngII), respectively, showing left ventricular hypertrophy in the heart from Gpx1<sup>-/-</sup> + AngII. THW/BW ratios in vehicle-treated wildtype and Gpx1<sup>-/-</sup> mice were similar (Figure 2E). THW/BW from wildtype mice treated with AngII was not significantly larger than wildtype mice treated with vehicle. Gpx1<sup>-/-</sup> + AngII hearts however, were significantly larger than Gpx1<sup>-/-</sup> + vehicle ( $p < 0.05$ ) and wildtype + AngII (21 % larger,  $p < 0.05$ , Figure 2E).

### Echocardiographic Measurement of Cardiac Hypertrophy and Function

**Diastolic Interventricular Septum (IVSTd)**—IVSTd at day 0 did not vary among treatment groups or strains (Figure 3A). In addition, IVSTd in vehicle-treated wildtype and Gpx1<sup>-/-</sup> mice did not increase from day 0 to 7. AngII treatment however, significantly elevated IVSTd in the Gpx1<sup>-/-</sup> group (day 7) versus its vehicle control. This elevation was significantly greater than that observed in the AngII-treated wildtype group ( $p < 0.05$ ).

**Measurements of Left Ventricular Mass**—At day 0, LV mass was not different among the treatment groups and strains (Figure 3B). LV mass did not change significantly in

vehicle-treated wildtype and Gpx1<sup>-/-</sup> mice (day 0 to 7). AngII treatment resulted in elevation in LV mass in mice from both strains ( $p < 0.05$ ) and this increase in LV mass by AngII was significantly greater in Gpx1<sup>-/-</sup> vs. wildtype groups at day 7 ( $p < 0.05$ ).

**Cardiac Shortening Fraction**—Cardiac shortening fraction (SF) did not vary significantly at day 0 among all groups (Figure 3C). SF did not change comparing day 7 with day 0 in wildtype + vehicle, wildtype + AngII, or Gpx1<sup>-/-</sup> + vehicle mice. SF was significantly reduced (13 %) after 7 days in AngII-treated Gpx1<sup>-/-</sup> mice ( $p < 0.05$ ). Moreover, at day 7 there was a significantly lower SF in AngII-treated Gpx1<sup>-/-</sup> mice compared to wildtype + AngII and both vehicle-treated groups ( $p < 0.05$ ).

**Measurements of Cardiac Chamber Dimensions**—Baseline (day 0) left ventricular end-systolic and end-diastolic dimension (LVDs or LVDd) did not differ among the treatment groups. At 7 days, in vehicle-treated wildtype and Gpx1<sup>-/-</sup> mice neither LVDs [ $1.15 \pm 0.03$  mm (wildtype) vs.  $1.16 \pm 0.03$  mm (Gpx1<sup>-/-</sup>)] nor LVDd [ $2.41 \pm 0.06$  mm (wildtype) vs.  $2.42 \pm 0.05$  mm (Gpx1<sup>-/-</sup>)] were significantly different. AngII had no significant effect on LVDd in either strain ( $2.45 \pm 0.10$  mm vs.  $2.46 \pm 0.11$  mm for wildtype and Gpx1<sup>-/-</sup>, respectively). Likewise AngII had no effect on LVDs in wildtype vs. Gpx1<sup>-/-</sup> ( $1.17 \pm 0.05$  mm vs.  $1.29 \pm 0.10$  mm, respectively).

**Myocyte Cross-sectional Area (MCSA) and Interstitial Collagen Fraction (ICF)**—MCSA did not differ between vehicle-treated wildtype and Gpx1<sup>-/-</sup> mice (Figure 4 A–B, E). AngII significantly increased MCSA in both strains ( $p < 0.05$ ) (Figure 4 C–D, E). Importantly, hypertrophy as measured by MCSA was greater in Gpx1<sup>-/-</sup> mice than wildtype ( $p < 0.05$ ). Representative images showing interstitial collagen in each group are illustrated in Figure 5 A – D. ICF was measured at  $3.8 \pm 0.2$  % in wildtype + vehicle; AngII significantly increased ICF to  $11 \pm 1.2$  % ( $p < 0.001$ , Fig. 5E). Similar collagen deposition was observed in Gpx1<sup>-/-</sup> mice. That is, ICF was  $4.0 \pm 0.2$  % in Gpx1<sup>-/-</sup> + vehicle and AngII elevated it to  $12 \pm 2.0$  % ( $p < 0.05$ ; Fig. 5E). The data showed no strain differences at basal conditions or after AngII.

**Vascular Remodeling**—Masson trichrome staining revealed similar aortic wall thickness (Wm/L ratio) in wildtype and Gpx1<sup>-/-</sup> mice treated with vehicle (Figure 6, left panel). Ang II significantly increased Wm/L ratio compared to both vehicle groups with no difference between strains ( $p < 0.001$ ). Aortic medial cross-sectional area (CSA) was similar between wildtype + vehicle and Gpx1<sup>-/-</sup> + vehicle mice ( $94.1 \pm 4.04$  and  $92 \pm 3.2 \times 10^3 \mu\text{m}^2$ , respectively) (Figure 6, right panel). AngII significantly enhanced CSA in both wildtype and Gpx1<sup>-/-</sup> mice ( $133 \pm 8.23$  and  $115 \pm 6.33$ , respectively) with no significant difference between strains.

**Assessment of Glutathione Peroxidase Activity and Protein Levels**—Gpx activity was measured in aortas as well as heart homogenates. In aortas of wildtype mice, Gpx activity was  $0.28 \pm 0.14$  mU/mg in vehicle-treated animals while it was  $0.47 \pm 0.24$  mU/mg in AngII-treated animals. In aortas of Gpx1<sup>-/-</sup> mice the Gpx activity was below the detection limit of the assay under both treatment conditions. In the case of heart homogenates, Western blots were used to assess protein levels and corroborate previously published findings showing a 10 fold decrease in Gpx1<sup>-/-</sup> compared to wildtype<sup>11</sup>. As expected, the levels of Gpx1 in Gpx1<sup>-/-</sup> animals were undetectable compared to robust levels in wildtype mice, both for vehicle or AngII-treated animals (Supplemental Figure S1). The data show a major reduction of vascular and cardiac Gpx1 from wildtype to knockout mice, corroborating previous findings by Ho et al which demonstrated a 10-fold decrease in Gpx1 in Gpx1<sup>-/-</sup> mice compared to wildtype<sup>11</sup>.

## DISCUSSION

Gpx1 is suggested to play an important role in moderating H<sub>2</sub>O<sub>2</sub> under pathological conditions<sup>11</sup>. In non-stressed heterozygous Gpx1 knockout mice, elevated ROS and oxidative stress in cardiovascular tissue is associated with ROS-mediated endothelial dysfunction<sup>12</sup>. Since AngII is a prototype stimulant of H<sub>2</sub>O<sub>2</sub> in heart and aorta, we hypothesized that in AngII-infused mice, deletion of Gpx1 would potentiate blood pressure elevation and both cardiac and aortic hypertrophy. Previously, the role of Gpx1 in hypertension and its effects on cardiac and vascular remodeling had not been studied. Here, using a Gpx1-knockout mouse model characterized by suppressed levels of Gpx activity and protein<sup>11</sup>, we provide anatomical (heart weight), morphological (LV mass and posterior wall thickness by echocardiography) and histological (myocyte cross-sectional area) evidence of enhanced AngII-induced LV hypertrophy in Gpx1<sup>-/-</sup> mice, despite no difference in blood pressure between AngII-treated wildtype and Gpx1<sup>-/-</sup> mice. In contrast to the heart, AngII-induced hypertrophy was not enhanced in Gpx1<sup>-/-</sup> aortas. Furthermore, preliminary data indicated a rise in ANP levels in Gpx1<sup>-/-</sup> mice consistent with enhanced hypertrophy in this strain (data not shown). Taken together, our results reveal a novel observation of a unique cardiac hypertrophy and dysfunction in Gpx1<sup>-/-</sup> mice.

### Mean Arterial Blood Pressure Measurements

AngII increased MABP compared to vehicle-treated mice of both strains. In light of a reported endothelial dysfunction in Gpx1<sup>-/-</sup> mice<sup>12</sup> and findings that Gpx1 deletion enhances AngII-induced impairments of vasodilatation<sup>16</sup>, a greater elevation in MABP after AngII might have been predicted. However, no difference was observed between the strains, possibly attributable to the existence of countervailing mechanisms affecting blood pressure. Importantly, this absence of a blood pressure difference between strains highlights a critical dissociation between MABP, increased cardiac hypertrophy and diminished function in response to AngII in Gpx1<sup>-/-</sup>. Thus our observations challenge the notion that AngII's effects on LV hypertrophy are simply pressor dependent<sup>17</sup>.

### Measurements of Cardiac Hypertrophy and Function

Total heart to body weight ratios did not increase significantly in wildtype animals after 7 days of AngII. This is not surprising given the short duration of AngII infusion. However, a significantly larger heart weight was observed in AngII-infused Gpx1<sup>-/-</sup> mice. This difference between strains was also clearly demonstrated histologically and echocardiographically. LV mass and MCSA were markedly higher in both AngII groups and further enhanced in Gpx1<sup>-/-</sup>. Furthermore, a significantly enhanced IVSTd was observed in Gpx1<sup>-/-</sup>, further supporting enhanced AngII susceptibility in Gpx1<sup>-/-</sup> vs. wildtype.

To further test for an effect of Gpx1 knockout on cardiac function, changes in left ventricular end-systolic and end-diastolic dimension were examined. We observed no changes in LVDD among the treatment groups. Although in wildtype LVDs did not change with AngII, there was a tendency for an increase in LVDs in Gpx1<sup>-/-</sup> treated with AngII. However the data did not reach statistical significance. Despite this, we observed a 13 % decrease in shortening fraction in Gpx1<sup>-/-</sup> mice treated with AngII. This decrease is considered a significant decrease in cardiac performance and might be viewed as a harbinger of more advanced dysfunction, highlighting the potentially important clinical significance of our findings. In fact, reduced Gpx1 activity in humans may be an important cardiac risk factor, since it has been shown that in patients with coronary heart disease lower Gpx1 is associated with an increased risk of cardiovascular events<sup>18</sup>.

Myocardial fibrosis is a pathological condition associated with cardiac hypertrophy and dysfunction and AngII's ability to increase cardiac interstitial collagen *via* ROS has been reported<sup>19</sup>. Thus, we also examined whether left ventricular cardiac ICF is enhanced in Gpx1<sup>-/-</sup> mice and could explain the early change in SF. In contrast to the report by Forgione *et al.* showing increased cardiac matrix in mice whose Gpx1 was partly compromised<sup>12</sup>, we did not observe enhanced collagen deposition in Gpx1<sup>-/-</sup> mice. Two possible explanations for the lack of effect of AngII in our study include (a) increased ROS did not rise to levels capable of enhancing AngII's effect on fibrosis; and/or (b) longer periods of elevated ROS may be necessary to sustain such an enhancement. Moreover, genetic background differences of heterozygous *vs.* homozygous knockouts, as well as their controls, could have contributed to the discrepancy.

Gpx1<sup>-/-</sup> mice treated with AngII exhibited a significantly decreased SF compared to controls. Theoretically, this functional change might be attributed to ROS-mediated hypertrophy leading to cardiac dysfunction and failure<sup>20</sup>. However, in the present study the rapid development of LV dysfunction in Gpx1<sup>-/-</sup> is likely to have resulted from a direct adverse cardiac cell effect of H<sub>2</sub>O<sub>2</sub>. In fact, previous studies showed that ROS including H<sub>2</sub>O<sub>2</sub> accelerate contractile dysfunction of the heart<sup>20, 21</sup>. Detrimental effects of H<sub>2</sub>O<sub>2</sub> include intracellular acidosis and electromechanical dysfunction, alterations in cardiac action potential, and contractile force inhibition<sup>22, 23</sup>. None of the differences observed can be attributed to changes in angiotensin II type 1 receptor as its levels did not vary among treatment groups (Supplemental Fig. S2).

Two reports challenge the role of antioxidant defenses in cardiac dysfunction and/or heart failure. Dieterich *et al.*<sup>24</sup> report an increased catalase activity in human end-stage heart failure. These data may be interpreted to contradict our findings that reduced antioxidant defenses contribute to cardiac dysfunction. However, as the authors point out, increased catalase activity may compensate for elevated ROS at this late stage of the disease. A second study by Baumer *et al.* reports the opposite<sup>25</sup>. That is, catalase activity is reportedly decreased in end-stage heart failure, consistent with our hypothesis that decreased antioxidant protection leads to dysfunction. Importantly, the study did not examine catalase activity at earlier time points and thus it is not possible to know whether compromised antioxidant defenses early in human disease contributes to heart failure. At this juncture, therefore, not enough evidence is available to solve this controversy. Moreover, caution should be taken in extrapolating findings in the mouse to human disease, especially considering that our findings are not related to chronic heart failure.

### Lack of Effect of Gpx1 Deficiency on Vascular Remodeling

Vascular medial hypertrophy in response to AngII is mediated, in part, by ROS<sup>15, 26</sup>. Thus we expected that in Gpx1<sup>-/-</sup> *vs.* wildtype, AngII-induced medial hypertrophy would be enhanced. However, our data showed no difference in AngII-induced hypertrophy between the strains as assessed by wall-to-lumen ratio and cross sectional area. These data are noteworthy since they highlight enhanced cardiac hypertrophy in Gpx1<sup>-/-</sup> mice in the absence of a change in vascular medial hypertrophy. The data indicate an accelerated cardiac response to Gpx 1 deficiency or enhanced cardiac sensitivity to smaller ROS increases compared to aorta.

In conclusion, left ventricular hypertrophy and dysfunction were accelerated in AngII-treated Gpx1<sup>-/-</sup> mice. These effects were not associated with increases in collagen deposition and were independent of blood pressure levels. No changes in vascular hypertrophy were observed, indicating a greater role of Gpx1 in cardiac *vs.* vascular protection. Our results demonstrate that Gpx1<sup>-/-</sup> mouse hearts are more susceptible to

dysfunction and further support the significance of antioxidant defense by Gpx1 in cardiac remodeling and function.

**Perspectives**—Hypertension and ventricular hypertrophy are major risk factors for cardiac dysfunction and congestive heart failure. Oxidative stress is an important mechanism involved in cardiovascular disease. ROS trigger signaling pathways that lead to cell proliferation, dysfunction and death as well as release of pro-inflammatory mediators that promote cardiovascular injury. Under physiological conditions, ROS is controlled by intrinsic antioxidant systems including Gpx1. In this study, we demonstrate that lack of Gpx1 promotes AngII-induced left ventricular hypertrophy, dilatation and dysfunction, supporting a pathophysiological role of ROS in the heart. The data further support the concept that antioxidant therapy may benefit the heart. Large prospective and randomized clinical trials failed to demonstrate clinical benefits of antioxidants on blood pressure and end-organ damage. Although the reasons for these outcomes are not clear, there are noteworthy limitations to those studies including the doses and form of antioxidants chosen, pre-existing cardiovascular conditions, trial design, and other medications administered to enrolled patients. Future studies will require a more focused and rational approach to targeting ROS rather than emphasizing the use of scavengers which may not be as efficacious or discriminating in their effects.

## Supplementary Material

Refer to Web version on PubMed Central for supplementary material.

## Acknowledgments

The authors would like to thank Dr. Imad Al Ghouleh for critical review of the manuscript.

### Sources of Funding

This work was supported by NIH grants HL55425 and HL28982 and the Fund for Henry Ford Hospital. Noelia Ardanaz was also supported by an American Heart Association Fellowship 0520056Z. PJP is an Established Investigator of the American Heart Association.

## References

1. Gardin JM, McClelland R, Kitzman D, Lima JA, Bommer W, Klopfenstein HS, Wong ND, Smith VE, Gottdiener J. M-mode echocardiographic predictors of six- to seven-year incidence of coronary heart disease, stroke, congestive heart failure, and mortality in an elderly cohort (the Cardiovascular Health Study). *Am J Cardiol.* 2001; 87:1051–1057. [PubMed: 11348601]
2. Verdecchia P, Porcellati C, Reboldi G, Gattobigio R, Borgioni C, Pearson TA, Ambrosio G. Left ventricular hypertrophy as an independent predictor of acute cerebrovascular events in essential hypertension. *Circulation.* 2001; 104:2039–2044. [PubMed: 11673343]
3. Frohlich ED. Overview of hemodynamic and non-hemodynamic factors associated with left ventricular hypertrophy. *J Mol Cell Cardiol.* 1989; 21:3–10. [PubMed: 2534139]
4. Hanevold C, Waller J, Daniels S, Portman R, Sorof J. The effects of obesity, gender, and ethnic group on left ventricular hypertrophy and geometry in hypertensive children: a collaborative study of the International Pediatric Hypertension Association. *Pediatrics.* 2004; 113:328–333. [PubMed: 14754945]
5. Cuspidi C, Muiesan ML, Valagussa L, Salvetti M, Di Biagio C, Agabiti-Rosei E, Magnani B, Zanchetti A. Comparative effects of candesartan and enalapril on left ventricular hypertrophy in patients with essential hypertension: the candesartan assessment in the treatment of cardiac hypertrophy (CATCH) study. *J Hypertens.* 2002; 20:2293–2300. [PubMed: 12409969]
6. Malmqvist K, Ohman KP, Lind L, Nystrom F, Kahan T. Long-term effects of irbesartan and atenolol on the renin-angiotensin-aldosterone system in human primary hypertension: the Swedish



- Irbesartan Left Ventricular Hypertrophy Investigation versus Atenolol (SILVHIA). *J Cardiovasc Pharmacol.* 2003; 42:719–726. [PubMed: 14639093]
7. Ardanaz N, Pagano PJ. Hydrogen peroxide as a paracrine vascular mediator: regulation and signaling leading to dysfunction. *Exp Biol Med (Maywood.)*. 2006; 231:237–251. [PubMed: 16514169]
  8. Swift LM, Sarvazyan N. Localization of dichlorofluorescein in cardiac myocytes: implications for assessment of oxidative stress. *Am J Physiol Heart Circ Physiol.* 2000; 278:H982–H990. [PubMed: 10710368]
  9. Zhang Y, Griendling KK, Dikalova A, Owens GK, Taylor WR. Vascular hypertrophy in angiotensin II-induced hypertension is mediated by vascular smooth muscle cell-derived H<sub>2</sub>O<sub>2</sub>. *Hypertension.* 2005; 46:732–737. [PubMed: 16172434]
  10. Ursini F, Maiorino M, Brigelius-Floh R, Aumann KD, Roveri A, Schomburg D, Floh L. Diversity of glutathione peroxidases. *Methods Enzymol.* 1995; 252:38–53. [PubMed: 7476373]
  11. Ho YS, Magnenat JL, Bronson RT, Cao J, Gargano M, Sugawara M, Funk CD. Mice deficient in cellular glutathione peroxidase develop normally and show no increased sensitivity to hyperoxia. *J Biol Chem.* 1997; 272:16644–16651. [PubMed: 9195979]
  12. Forgione MA, Cap A, Liao R, Moldovan NI, Eberhardt RT, Lim CC, Jones J, Goldschmidt-Clermont PJ, Loscalzo J. Heterozygous cellular glutathione peroxidase deficiency in the mouse. Abnormalities in vascular and cardiac function and structure. *Circulation.* 2002; 106:1154–1158. [PubMed: 12196344]
  13. Rhaleb NE, Yang XP, Nanba M, Shesely EG, Carretero OA. Effect of Chronic Blockade of the Kallikrein-Kinin System on the Development of Hypertension in Rats. *Hypertension.* 2001; 37:121–128. [PubMed: 11208766]
  14. Yang XP, Liu YH, Rhaleb NE, Kurihara N, Kim HE, Carretero OA. Echocardiographic assessment of cardiac function in conscious and anesthetized mice. *Am J Physiol.* 1999; 277:H1967–H1974. [PubMed: 10564153]
  15. Liu J, Ormsby A, Oja-Tebbe N, Pagano PJ. Gene transfer of NAD(P)H oxidase inhibitor to the vascular adventitia attenuates medial smooth muscle hypertrophy. *Circ Res.* 2004; 95:587–594. [PubMed: 15308582]
  16. Chrissobolis S, Didion SP, Kinzenbaw DA, Schrader LI, Dayal S, Lentz SR, Faraci FM. Glutathione peroxidase-1 plays a major role in protecting against angiotensin II-induced vascular dysfunction. *Hypertension.* 2008; 51:872–877. [PubMed: 18299484]
  17. Reudelhuber TL, Bernstein KE, Delafontaine P. Is angiotensin II a direct mediator of left ventricular hypertrophy? Time for another look. *Hypertension.* 2007; 49:1196–1201. [PubMed: 17452509]
  18. Blankenberg S, Rupprecht HJ, Bickel C, Torzewski M, Hafner G, Tiret L, Smieja M, Cambien F, Meyer J, Lackner KJ. Glutathione peroxidase 1 activity and cardiovascular events in patients with coronary artery disease. *N Engl J Med.* 2003; 349:1605–1613. [PubMed: 14573732]
  19. Johar S, Cave AC, Narayanapanicker A, Grieve DJ, Shah AM. Aldosterone mediates angiotensin II-induced interstitial cardiac fibrosis via a Nox2-containing NADPH oxidase. *FASEB J.* 2006; 20:1546–1548. [PubMed: 16720735]
  20. Seddon M, Looi YH, Shah AM. Oxidative stress and redox signalling in cardiac hypertrophy and heart failure. *Heart.* 2007; 93:903–907. [PubMed: 16670100]
  21. Brenner DA, Jain M, Pimentel DR, Wang B, Connors LH, Skinner M, Apstein CS, Liao R. Human amyloidogenic light chains directly impair cardiomyocyte function through an increase in cellular oxidant stress. *Circ Res.* 2004; 94:1008–1010. [PubMed: 15044325]
  22. Ferdinandy P, Danial H, Ambrus I, Rothery RA, Schulz R. Peroxynitrite is a major contributor to cytokine-induced myocardial contractile failure. *Circ Res.* 2000; 87:241–247. [PubMed: 10926876]
  23. Loh SH, Tsai CS, Tsai Y, Chen WH, Hong GJ, Wei J, Cheng TH, Lin CI. Hydrogen peroxide-induced intracellular acidosis and electromechanical inhibition in the diseased human ventricular myocardium. *Eur J Pharmacol.* 2002; 443:169–177. [PubMed: 12044806]

24. Dieterich S, Bieligg U, Beulich K, Hasenfuss G, Prestle J. Gene Expression of Antioxidative Enzymes in the Human Heart : Increased Expression of Catalase in the End-Stage Failing Heart. *Circulation*. 2000; 101:33–39. [PubMed: 10618301]
25. Baumer AT, Flesch M, Wang X, Shen Q, Feuerstein GZ, Bohm M. Antioxidative enzymes in human hearts with idiopathic dilated cardiomyopathy. *J Mol Cell Cardiol*. 2000; 32:121–130. [PubMed: 10652196]
26. Wang HD, Xu S, Johns DG, Du Y, Quinn MT, Cayatte AJ, Cohen RA. Role of NADPH oxidase in the vascular hypertrophic and oxidative stress response to angiotensin II in mice. *Circ Res*. 2001; 88:947–953. [PubMed: 11349005]

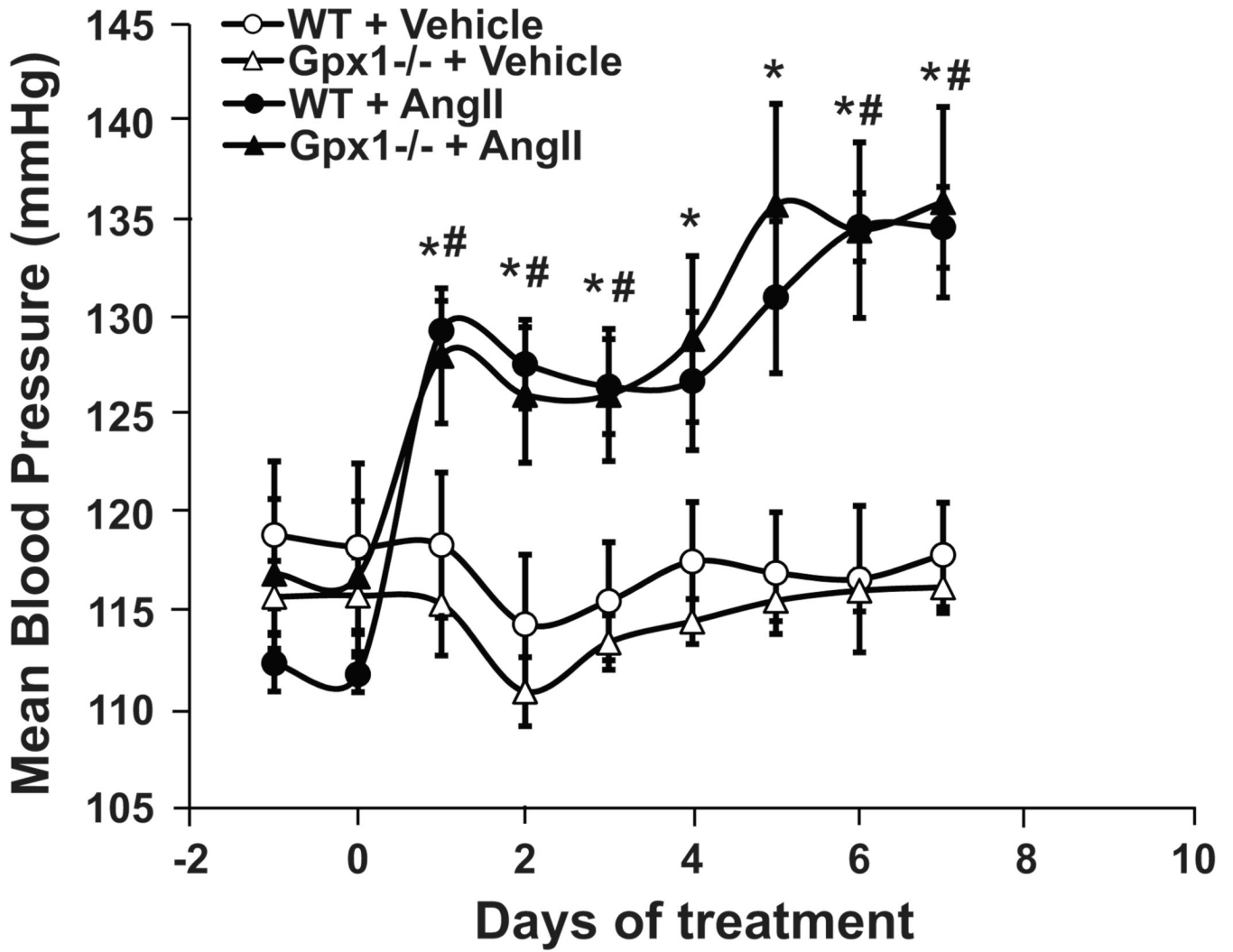


**Figure 1. MABP changes in wildtype and Gpx1<sup>-/-</sup> mice**

MABP was measured by radio-telemetry from days -1 to 7 in wildtype and Gpx1<sup>-/-</sup> mice treated with AngII (521 ng/kg\*min, *s.c.*) or vehicle for 7 d. Data are expressed as mean  $\pm$  SEM. #  $p < 0.05$  vs. wildtype + vehicle; \*  $p < 0.05$  vs. Gpx1<sup>-/-</sup> + vehicle ( $n = 6 - 7$ ).

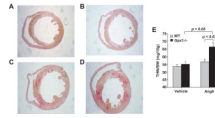


**Figure 2. Comparison of cardiac mass in wildtype vs. Gpx1<sup>-/-</sup> mice**

Hearts were harvested after 7 days treatment with vehicle or AngII (521 ng/kg\*min, *s.c.*). Representative cross-sections of hearts from wildtype + vehicle (A), Gpx1<sup>-/-</sup> + vehicle (B), wildtype + AngII (C) and Gpx1<sup>-/-</sup> + AngII (D) stained with picosirius red. Total Heart Weight/ Body Weight (THW/BW) ratio was tabulated for hearts from vehicle- and AngII-treated wildtype and Gpx1<sup>-/-</sup> mice (E). Data are expressed as mean  $\pm$  SEM ( $n = 9 - 10$ ).

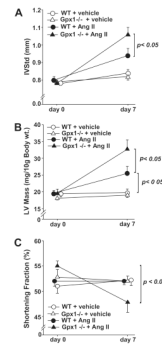


### Figure 3. Echocardiographic Measurement of Cardiac Hypertrophy and Function

A). Changes in diastolic interventricular septum thickness (IVSTd) in wildtype and Gpx1<sup>-/-</sup> mice. Values were quantified from 3 separate M-mode measurements by echocardiography on conscious mice before (day 0) and after vehicle or AngII treatment (day 7). B) Changes in left ventricular mass (LV mass) in wildtype mice and Gpx1<sup>-/-</sup> mice treated with vehicle or AngII. Measurements were performed using echocardiography on conscious mice before (day 0) and after vehicle or AngII (day 7). C) Comparison of shortening fraction (SF) in wildtype and Gpx1<sup>-/-</sup> mice. Echocardiographic measurements were taken before (day 0) and after vehicle or AngII treatment (day 7). Data expressed as mean  $\pm$  SEM ( $n = 9 - 10$ ) (\*  $p < 0.05$ , \*\*  $p < 0.001$ ).

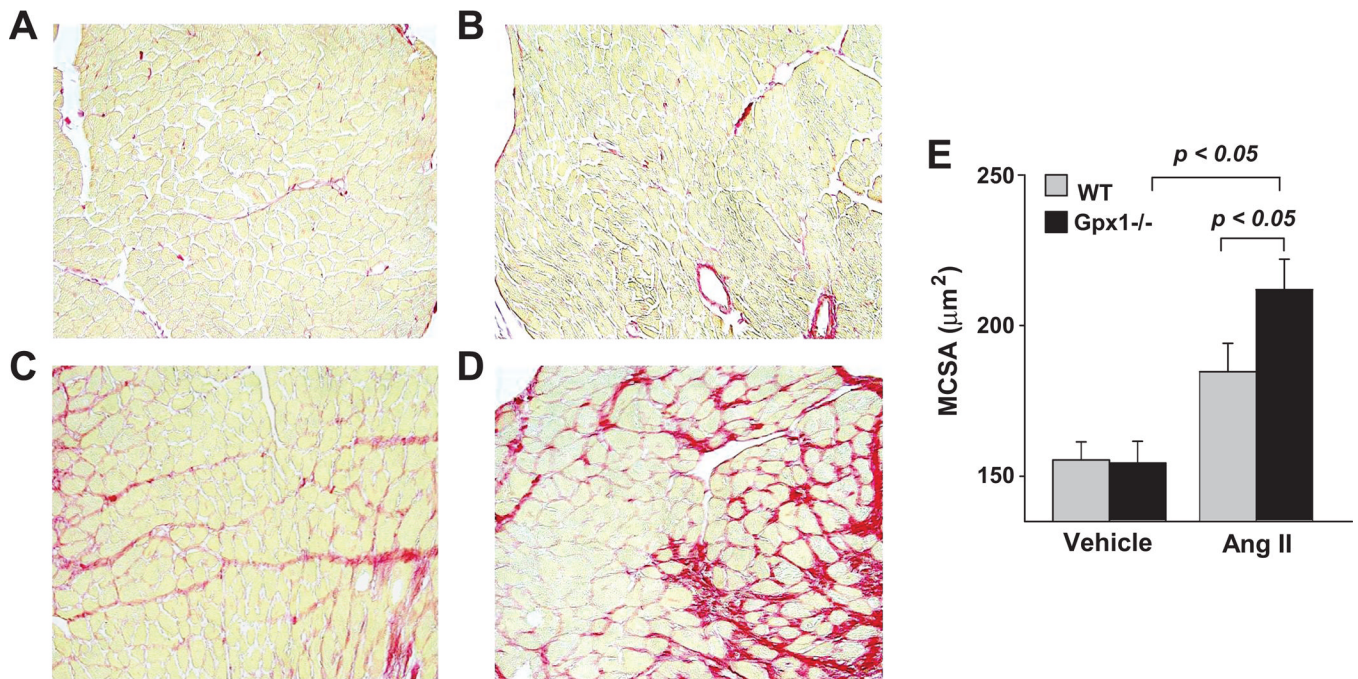


**Figure 4. Left ventricular myocyte cross-sectional area (MCSA) in wildtype mice and Gpx1 <sup>-/-</sup> mice**

Mice were treated with AngII or vehicle and cardiac sections were evaluated for MCSA. Panels show representative heart sections from wildtype + vehicle (A), Gpx1 <sup>-/-</sup> + vehicle (B), wildtype + AngII (C), and Gpx1 <sup>-/-</sup> + AngII (D) mice. Picosirius red stain was used to demarcate myocytes as well as stain for collagen MCSA was measured after 7 days of vehicle or Ang II treatment. MCSA (µm<sup>2</sup>) was digitally measured and expressed as mean ± SEM (E) (*n* = 9 – 10). Original magnification ×200.

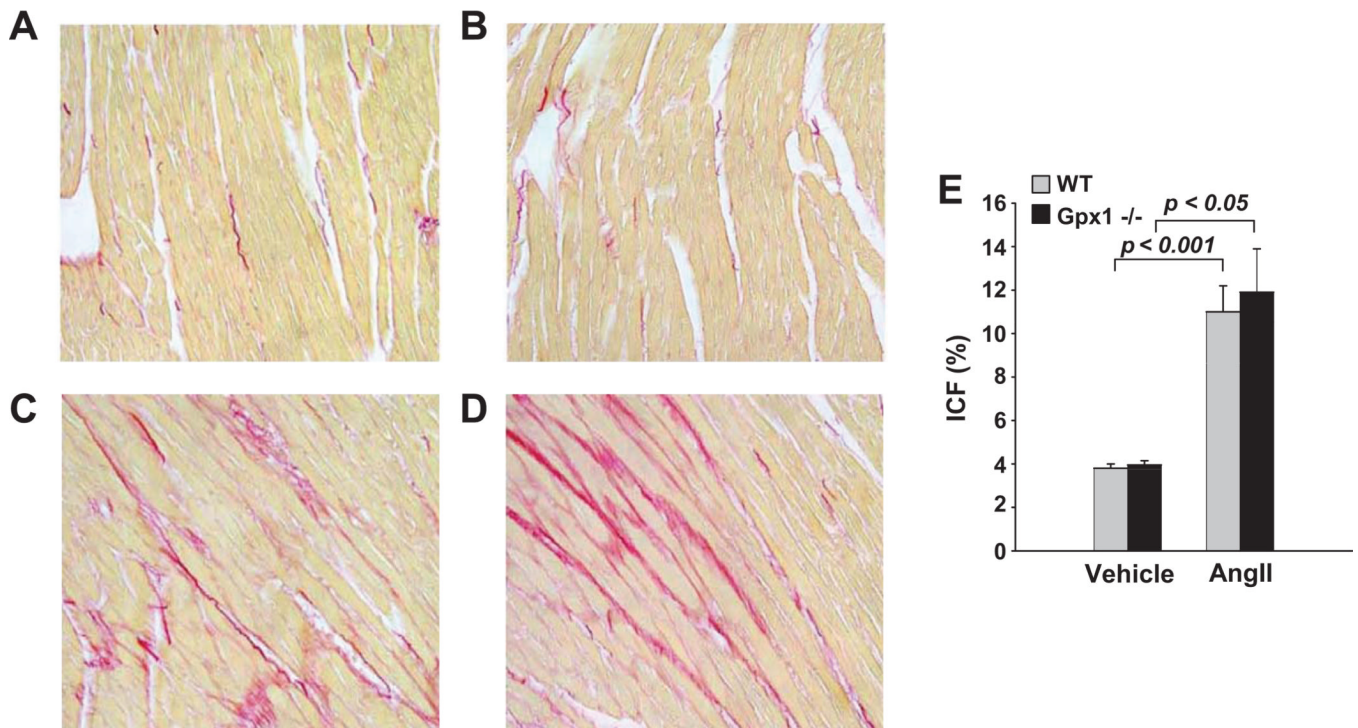


**Figure 5. Left ventricular interstitial collagen fraction (ICF %) in wildtype mice and Gpx1<sup>-/-</sup> mice**

Mice were treated with AngII or vehicle and cardiac sections were stained with picrosirius red. Panels show representative heart sections from wildtype + vehicle (A), Gpx1<sup>-/-</sup> + vehicle (B), wildtype + AngII (C), and Gpx1<sup>-/-</sup> + AngII (D) mice. ICF % of total area was digitally measured and expressed as mean  $\pm$  SEM (E) ( $n = 9 - 10$ ). Original magnification  $\times 200$ .

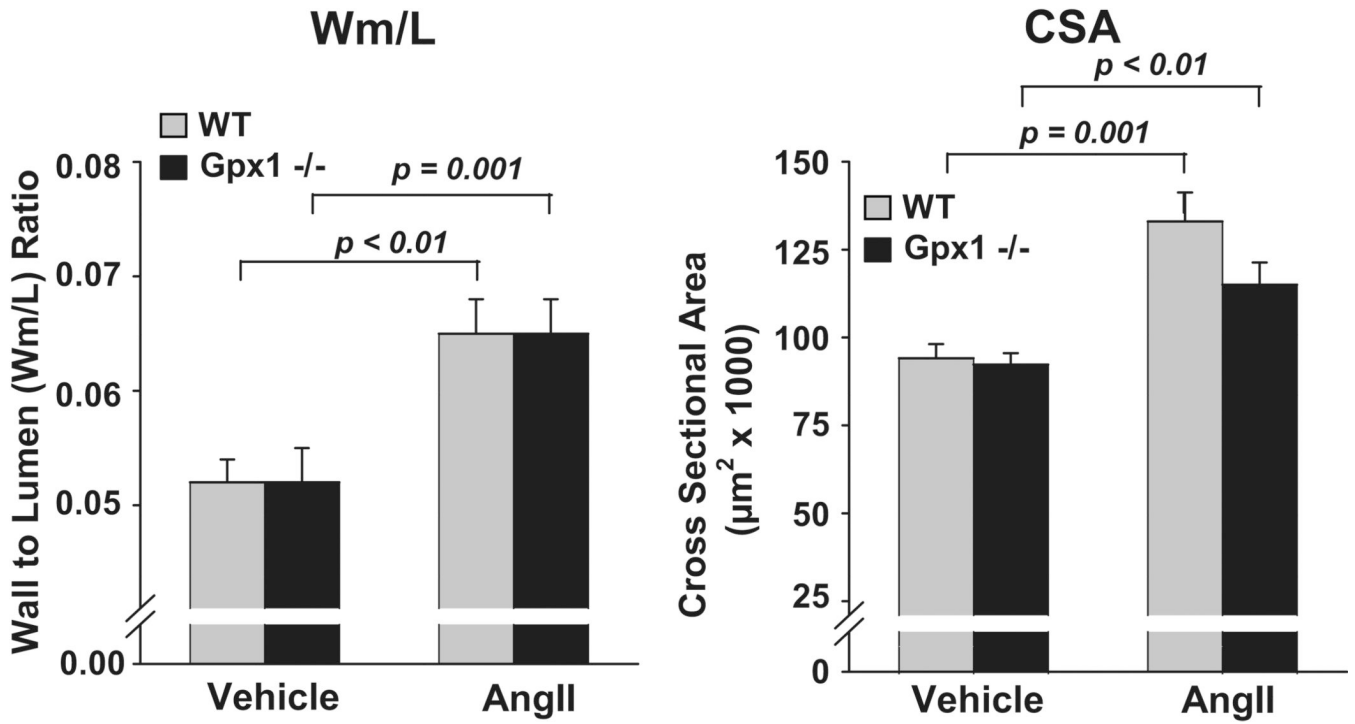


**Figure 6. Comparisons of aortic wall thickness to lumen ratio (Wm/L) and cross sectional area (CSA) in wildtype mice and Gpx1<sup>-/-</sup> mice**  
 Mice were treated with AngII or vehicle for 7 days. Thoracic aortas were stained with Masson Trichrome and parameters digitally obtained by image analysis. Data are expressed as mean ± SEM. \*  $p < 0.05$  vs. vehicle ( $n = 9 - 10$ ).